Spin Quantum Heat Engine Quantified by Quantum Steering

Wentao Ji[1,3,*] Zihua Chai[1,3,*] Mengqi Wang,[1,3,*] Yuhang Guo,[1,3] Xing Rong,[1,3] Fazhan Shi[1,3] Changliang Ren[2,†]
Ya Wang[1,3,‡] and Jiangfeng Du[1,3,§]

[1]*CAS Key Laboratory of Microscale Magnetic Resonance and School of Physical Sciences,
University of Science and Technology of China, Hefei 230026, China*
[2]*Key Laboratory of Low-Dimensional Quantum Structures and Quantum Control of Ministry of Education,
Key Laboratory for Matter Microstructure and Function of Hunan Province, Department of Physics and
Synergetic Innovation Center for Quantum Effects and Applications, Hunan Normal University, Changsha 410081, China*
[3]*CAS Center for Excellence in Quantum Information and Quantum Physics, University of Science and
Technology of China, Hefei 230026, China*

Following the rising interest in quantum information science, the extension of a heat engine to the quantum regime by exploring microscopic quantum systems has seen a boon of interest in the last decade. Although quantum coherence in the quantum system of the working medium has been investigated to play a nontrivial role, a complete understanding of the intrinsic quantum advantage of quantum heat engines remains elusive. We experimentally demonstrate that the quantum correlation between the working medium and the thermal bath is critical for the quantum advantage of a quantum Szilárd engine, where quantum coherence in the working medium is naturally excluded. By quantifying the nonclassical correlation through quantum steering, we reveal that the heat engine is quantum when the demon can truly steer the working medium. The average work obtained by taking different ways of work extraction on the working medium can be used to verify the real quantum Szilárd engine.

Exploring thermodynamics at the quantum level opens up intriguing possibilities, including testing information theory in the quantum regime [1–9], the development of quantum fluctuation theorems [10–19], and the realization of microscopic quantum heat engines (QHEs) [20–33]. In particular, a microscopic QHE may operate more efficiently for work extraction than its classical counterpart by exploring the quantum effect. Over the years, enthusiastic interest has been devoted to implementing QHEs by controlling nonequilibrium dynamics in various microscopic systems, such as atomic systems [20,21], trapped ions [22], solid-state spin systems [23,24], photonic systems [25], single-electron transistors [26–29], nuclear magnetic resonance [30–32], superconducting qubits [33], among others. As quantum coherence is an intrinsic property for quantum systems, previous studies have intensively investigated the role of quantum coherence by using single particles or few-level quantum systems as the working medium. Recently, some research shows this potential high efficiency [24,31,34–36], while the other investigations show that quantum coherence effects are generally detrimental to reaching bounds on the maximum efficiency and power of these efficient thermal engines [37–41]. Hence understanding the advantage of quantumness in QHEs qualitatively and quantitatively remains a central issue from both a fundamental and practical perspective of quantum thermodynamics [42].

In this Letter, we report an experimental demonstration of a quantum heat engine that can truly exhibit quantum advantage. By building a quantum Szilárd engine, where quantum correlation exists between the working medium and the thermal bath, we have conclusively identified quantum correlation as a source of quantum advantage for the QHE, since the reduced state of its working medium is a Gibbs state that naturally excludes the intrinsic coherence feature. By quantifying the correlation with quantum steering, we clearly show that an optimized steering-type inequality, which is expressed by the average work over different ways of work extraction on the working medium, can distinguish quantum Szilárd engines from classical heat engines. The more the quantum steering inequality is violated, the more average work the quantum Szilárd engine can output than its classical counterpart.

The Szilárd engine, proposed by Szilárd in [43,44], serves as a prototypical model for understanding the fundamental relation between thermodynamics and information science [5,6,8,45–47]. A conventional Szilárd engine consists of a single atom as the working medium, which is in the thermal equilibrium within a box [6]. The demon measures the atom's microstate and controls the single atom doing work, as shown in Fig. 1(a). To resemble the conventional Szilárd engine, we construct a modified Szilárd engine with a quantum system as a proof-of-principal demonstration. We use one qubit as the working
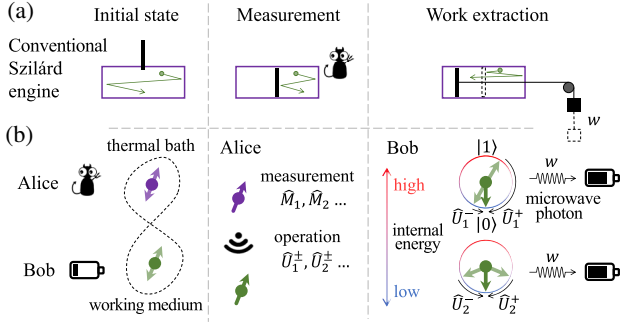
FIG. 1. Conventional and modified Szilárd engine. (a) For the conventional Szilárd engine, the working medium is a single atom that initially stayed in a thermal equilibrium state. A demon measures which half of the box the atom is in. If the atom is in the right half of the box, a movable shutter is put down in the middle. Then the shutter is hung to a load and extracts work from the atom. (b) For the modified Szilárd engine, both the working medium and the bath are resembled by a single spin qubit, respectively. Alice (the demon) prepares the initial state of the whole system, performs measurement $\hat{M}_i$ on the bath qubit, and tells Bob the operations $\hat{U}_i^{\pm}$ depending on the measurement outcomes ± 1. Bob implements the operations $\hat{U}_i^{\pm}$ on the working medium qubit to extract work from its internal energy.

medium, and another qubit as the bath. In equilibrium, the working medium is in a Gibbs state [6]

$$\rho_M^{\text{Gibbs}} = \frac{1+\eta}{2}|1\rangle\langle 1| + \frac{1-\eta}{2}|0\rangle\langle 0|, \qquad (1)$$

where $\eta = (e^{-\beta} - 1)/(e^{-\beta} + 1)$ and $\beta = 1/k_B T$. Because of its quantum nature, the modified Szilárd engine is fundamentally threefold different from its conventional counterpart in threefolds. First, direct quantum measurement of the working medium, in general, destroys its quantum state and disturbs the local thermodynamical situation, like changing the average energy of the working medium [9]. To avoid such disturbance, the demon instead can choose to perform the positive operator-valued measurement on the bath and communicate outcome-dependent energy-conserving operations to the working medium, enabling the subsequent work extraction [48]. Second, for a quantum system of the working medium, a statistical mixture of states allows for infinitely many different ensembles of pure states. Different decompositions may lead to different extraction ways. Lastly, in general, demonstrating quantum properties requires at least two measurements that do not commute with each other [42,49]. After taking these differences into account, Fig. 1(b) displays the prototypical model of our quantum Szilárd engine and the work extraction ways investigated in this Letter. The demon, named Alice, prepares the initial state of the Szilárd engine and decides the energy-conserving operations $\hat{U}_i^{\pm}$ depending on the outcomes of
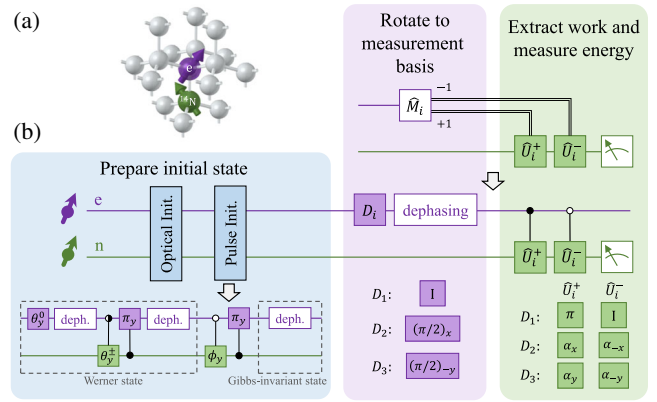

FIG. 2. Experimental circuit for implementing the modified Szilárd engine. (a) The experimental system: a nitrogen vacancy (NV) center in diamond. The bath and the working medium are resembled by the intrinsic electron spin and nitrogen nuclear spin of the NV center. (b) The quantum circuit for the experimental implementation. In the state preparation step, different circuits are used to prepare different types of correlated initial states. The circuit in the left dashed box is for the Werner states, and the right dashed box is for the Gibbs-invariant mixed states. $\theta_y^{0,\pm}$ and ϕ_y are rotations along y axis. The rotation angle and the dephasing processes are dependent on η and q. In the measurement step, depending on the decomposition $D_{i=1,2,3}$, the electron spin is measured with $\hat{M}_{1,2,3} = \sigma_{z,y,x}$. This is equivalently realized by the operations labeled by D_i (listed below), which rotates the measurement basis of $\hat{M}_i$ to the σ_z Pauli basis. Finally, the work is extracted by the controlled rotations $\hat{U}_i^{\pm}$ on the nuclear spin, and the final energy of the nuclear spin is measured [56].

the measurement $\hat{M}_i$. Bob implements the operations $\hat{U}_i^{\pm}$ on the working medium and extracts work from it.

We implement this prototypical quantum Szilárd engine with a nitrogen vacancy (NV) center in diamond. The intrinsic nuclear spin of nitrogen is used as the working medium, and the electronic spin of the NV center is used as the bath. High-fidelity spin manipulation [50,51], on-demand decoherence control [52] as well as optical readout of the spin state [53–55] make this quantum system well-suited for demonstrating microscopic heat engines [23] and understanding the underlying physics. The relevant quantum circuit consists of three steps, as shown in Fig. 2(b). The whole system is optically initialized into the $|00\rangle$ state and then prepared to a state with specific quantum correlation by a combination of microwave control of electron spin, radio-frequency control of nuclear spin, as well as controllable dephasing processes. The measurement-outcome-dependent operations are realized by the electron-spin-controlled rotation (CROT) gates on the nuclear spin. The measurements are realized by first rotating the electron spin to the corresponding basis and then dephasing the electron spin before implementing the CROT gates. The extracted work is obtained by reading out the nuclear spin state and calculating energy difference $W = \text{Tr}(\rho_{n,\text{init}}\hat{H}_M) - \text{Tr}(\rho_{n,\text{final}}\hat{H}_M)$, with the internal energy of the working medium $\hat{H}_M = |1\rangle\langle 1|$ [56].
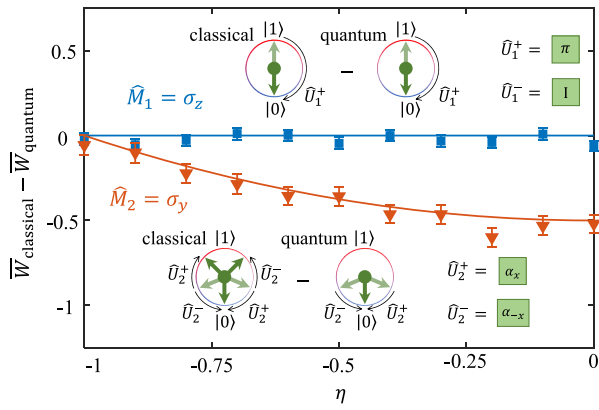
FIG. 3. Difference between work extracted from classical and quantum global states. The quantum (classical) global state is a pure entangled state ρ_1 (separable state ρ_2). The blue (red) data points are the work difference of measurement $\hat{M}_1 = \sigma_z$ ($\hat{M}_2 = \sigma_y$), with error bars representing one standard deviation. The solid lines are the theoretical predictions. For the $\hat{M}_1$ measurement, work extraction from both the classical and quantum global states are optimal, yielding the same extracted work. While for the $\hat{M}_2$ measurement, work extraction from the classical state is no longer optimal, and can extract less work than from the quantum global state.

In order to understand the effect of quantum correlation, we first consider two typical global quantum states giving the same thermalized local Gibbs state as illustrated in Eq. (1). The first state is a pure entangled state of $\rho_1 = |\psi\rangle\langle\psi|$ with $|\psi\rangle = \sqrt{[(1+\eta)/2]}|11\rangle + \sqrt{[(1-\eta)/2]}|00\rangle$, and the second state is a separable state of $\rho_2 = [(1+\eta)/2]|11\rangle\langle11| + [(1-\eta)/2]|00\rangle\langle00|$. From Bob's side, he cannot distinguish these two cases and will expect to extract the same work for the same extraction process. In both cases, Alice measures the bath qubit by $\hat{M}_1 = \sigma_z$ or $\hat{M}_2 = \sigma_y$, and chooses from operation $\hat{U}_1^+/\hat{U}_1^-$ or $\hat{U}_2^+/\hat{U}_2^-$ depending on the measurement result. For $\hat{M}_1$ measurement, $\hat{U}_1^+ = \sigma_x$ for the measurement result $+1$ and $\hat{U}_1^- = I$ for the measurement result -1. For $\hat{M}_2$ measurement, $\hat{U}_2^{\pm}$ are rotations around the $\pm x$ axis for an angle $\alpha = 2\arctan\sqrt{(1+\eta)/(1-\eta)}$ [56]. Figure 3 shows the experimentally extracted work difference between ρ_2 (classical) and ρ_1 (quantum). For work extraction with the $\hat{M}_1$ measurement, Bob finds no difference between these two Szilárd engines constructed by ρ_1 and ρ_2. The $\hat{U}_1^+/\hat{U}_1^-$ operations extract the largest amount of the work by flipping the working medium qubit to the lower energy $|0\rangle$ state. For the $\hat{M}_2$ measurement, Alice still provides Bob the optimal work extraction for state ρ_1, while for ρ_2 it is no longer optimal. Apparently, the average work of these two measurement-based extractions will unambiguously distinguish the Szilárd engines with and without specific quantum correlation. If the investigations only focus on the working medium itself, ignoring the bath-medium

correlation, or are limited to a single way of work extraction ($\hat{M}_1 = \sigma_z$ here), which is usually assumed in previous investigations [16], the effect of quantum correlation will be missing.

Some crucial questions are whether and when a Szilárd engine with quantum correlation can be distinguished from any classical Szilárd engines with the same Gibbs state of the working medium. A better classical strategy may exist for the classical Szilárd engine. However, the optimal average extracted work for such a classical Szilárd engine is bounded by the local statistical ensemble description, which is a local hidden state (LHS) model. If the average work output from a Szilárd engine is greater than the upper bound given by the LHS model, the quantumness of the Szilárd engine can be unambiguously identified. This is analogous to the identification of quantum steering, which is a special kind of quantum correlation [49,58]. Specifically, for the classical Szilárd engines with thermalized Gibbs states Eq. (1) on the working medium, suppose that Bob would like to extract work from three dichotomic pure state decompositions $D_{i=1,2,3}$, of which the bases are given by Bloch vectors $n_1^{\pm} = (0, 0, \pm 1)$, $n_2^{\pm} = (0, \mp\sqrt{1-\eta^2}, \eta)$, and $n_3^{\pm} = (\pm\sqrt{1-\eta^2}, 0, \eta)$, respectively. If Bob takes each work extraction D_i randomly with the probability c_i, the locally extracted work is bounded by

$$\overline{W}_{\text{LHS}}^{\text{opt}} = \frac{1}{2}\left(\eta + (c_2 + c_3)\eta^2 + \sqrt{c_1^2 + (c_2^2 + c_3^2)(1-\eta^2)}\right),$$

(2)

namely, the local work extraction bound [56]. A quantum strategy for Alice can be to measure $\hat{M}_{1,2,3} = \sigma_{z,y,x}$ according to the decomposition $D_{1,2,3}$ Bob wants to use, and then instruct Bob to perform the corresponding work extraction operation $\hat{U}_{1,2,3}^{\pm}$ depending on the measurement result ± 1. This strategy is optimal for the pure entangled state ρ_1, and guarantees the maximal extracted work $(1+\eta)/2$, exceeding the local work extraction bound. A genuine quantum Szilárd engine can therefore be defined by the violation of the work extraction inequality $\bar{W} \leq \bar{W}_{\text{LHS}}^{\text{opt}}$, which means Bob's average work output from such an engine is larger than what could be obtained from any classical Szilárd engine with the same Gibbs state of the working medium. It can clearly divide heat engines into two categories, quantum and classical, where no classical statistical description exists for quantum heat engines.

To demonstrate the classification of quantum and classical Szilárd engines, our experiment adopts the Gibbs-invariant mixed states and the Werner states as the global quantum state of the Szilárd engine. The Gibbs-invariant mixed states are $\rho_{\text{GI}} = q\rho_1 + (1-q)\rho_2$, where the parameter q tunes the system between the fully quantum case (ρ_1 at $q = 1$) and the fully classical case (ρ_2 at $q = 0$). For a given η, the reduced state of the working medium is always
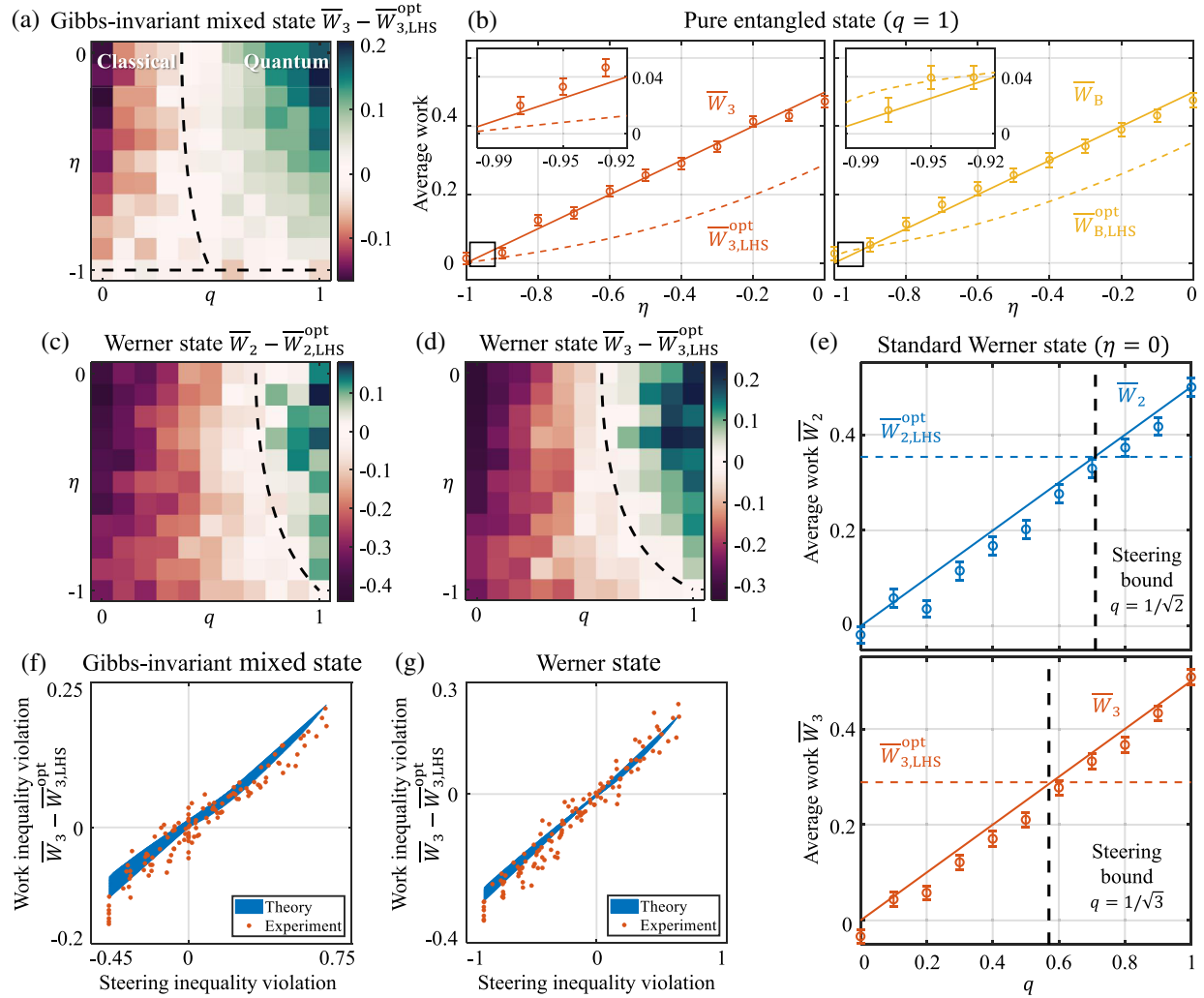
FIG. 4. Identification of quantumness with the work extraction inequality. (a) Violation of the work extraction inequality $\bar{W}_3$ for the Gibbs-invariant mixed states. The color indicates the difference between the extracted work and its local work extraction bound, with the white color indicates the boundary where the work extraction inequality is violated. The dashed black line is the theoretical prediction of the boundary. (b) Comparison between the extracted work and its local work extraction bound for the pure entangled states. The data points are experimental results of the extracted work, with the error bars representing one standard deviation, and the solid lines representing the theoretical predictions. The dashed lines are the local work extraction bound. The color of red represents the work extraction with $(c_1, c_2, c_3) = (1/3, 1/3, 1/3)$, and yellow represents the work extraction inequality proposed in [42]. From the insets, the extracted work of $\bar{W}_3$ violates its local work extraction bounds, whereas $\bar{W}_B$ doesn't, showing that work extraction inequality $\bar{W}_3$ is more effective than $\bar{W}_B$. (c),(d) Violation of the work extraction inequality $\bar{W}_2$ and $\bar{W}_2$ for the Werner states. (e) Comparison between the extracted work and its local work extraction bound for the standard Werner states. For the standard Werner states ($\eta = 0$), the work extraction inequalities can be violated when $q > 1/\sqrt{2}$ for $\bar{W}_2$ and $q > 1/\sqrt{3}$ for $\bar{W}_3$, as marked by the dashed black lines. This is consistent with the well-known linear steering inequalities [60]. (f),(g) Correspondence between quantum steering and work extraction inequality violation [61]. The experimental results in (a),(d) are plotted as the vertical axis of the data points, and the horizontal axis is the steering inequality violation calculated from the corresponding states. The clear positive correlation demonstrates the effectiveness of identifying quantum steering with work extraction inequalities.

the same Gibbs state, independent of the mixing parameter q, as also mentioned in [42]. For different η and q, we measure the average extracted work $\bar{W}_3$ ($c_1 = 1/3$, $c_2 = 1/3, c_3 = 1/3$), and the difference between $\bar{W}_3$ and the local work extraction bound $\bar{W}_{3,\text{LHS}}^{\text{opt}}$ is shown in Fig. 4(a). It is clearly shown that for some parameters the Szilárd engines can output more work than the local work

extraction bound $\bar{W}_{\text{LHS}}^{\text{opt}}$, excluding any classical description, hence, the quantum nature is revealed. The theoretical boundary of the quantum Szilárd engines is plotted as the dashed black line. For the line with $q = 1$, $\eta > -1$, the global state is the pure entangled state ρ_1. Given that any pure entangled state is steerable [58], we would expect the work extraction inequality to identify the quantumness over

the whole line, as shown in the left plot of Fig. 4(b). In the right plot of Fig. 4(b), the results for the work extraction inequality $\bar{W}_B$ as proposed in [42] are also displayed. As shown in the right inset, $\bar{W}_B$ fails to identify quantumness in this region, while in the left inset it is identified successfully, showing the advantage of the inequalities proposed here over $\bar{W}_B$ [42,58]. The other type of global state is the Werner state, which is the best-known class of mixed entangled states, and first revealed the difference between the notion of entanglement and Bell nonlocality [59]. For Werner states $\rho_w = q\rho_1 + [(1-q)/4]\mathrm{I} \otimes \mathrm{I}$ with different η and q, the average extracted work $\bar{W}_2$ ($c_1 = 1/2, c_2 = 1/2, c_3 = 0$) and $\bar{W}_3$ ($c_1 = 1/3, c_2 = 1/3, c_3 = 1/3$) are measured, as shown in Figs. 4(c) and 4(d). Especially, for standard Werner states ($\eta = 0$), the above work extraction inequalities can be violated when $q > 1/\sqrt{2}$ for $\bar{W}_2$ and $q > 1/\sqrt{3}$ for $\bar{W}_3$, as shown in Fig. 4(e). These results are consistent with the well-known linear steering inequalities [60], and strongly demonstrate that the task of clarifying the quantum Szilárd engine can be one-to-one mapped to the problem of identifying quantum steering when the system is standard Werner states. To further reveal the correspondence between quantum steering and the work extracted from the Szilárd engine, we plot the experimental work extraction inequality violation shown in Figs. 4(a) and 4(d) versus the steering inequality violation, which is derived from the all-versus-nothing proof of the steering paradox [61]. This steering inequality includes, naturally, the usual linear steering inequality [60] as a special case, and thus can detect more quantum states. As shown in Figs. 4(f) and 4(g), for both the Gibbs-invariant mixed states and the Werner states, the results show positive correlation, demonstrating that the work extraction inequality is an effective indicator for quantum steering between the working medium and the bath, hence, it correctly identifies the quantumness of the Szilárd engine.

Conclusions.—We have experimentally demonstrated a truly quantum Szilárd engine in diamond when the demon can "steer" the working medium where an optimized steering-type inequality that we derived can be violated. Our theoretical and experimental results show that a quantum heat engine which excludes the intrinsic coherence feature in the working medium, can truly exhibit quantum advantage. We hope our work triggers further studies to generalize our results to the other kind of quantum heat engines. Our Letter can be naturally extended to the case of the working medium with higher dimensions. In the future, it will be interesting to study these heat engines where the working medium is a higher dimensional system. The investigation of quantifying genuine high dimensional quantum steering [49,62] can benefit from it. As well, our research can stimulate the bloom of high-dimensional quantum steering.

*These authors contributed equally to this work.
†Corresponding author.
renchangliang@hunnu.edu.cn
‡Corresponding author.
ywustc@ustc.edu.cn
§Corresponding author.
djf@ustc.edu.cn

[1] R. Landauer, Irreversibility and heat generation in the computing process, IBM J. Res. Dev. 5, 183 (1961).

[2] E. T. Jaynes, Information theory and statistical mechanics, Phys. Rev. 106, 620 (1957).

[3] R. T. Cox, The algebra of probable inference, Am. J. Phys. 31, 66 (1963).

[4] C. H. Bennett, Notes on Landauer's principle, reversible computation, and Maxwell's demon, Stud. Hist. Phil. Sci. Part B 34, 501 (2003).

[5] M. B. Plenio and V. Vitelli, The physics of forgetting: Landauer's erasure principle and information theory, Contemp. Phys. 42, 25 (2001).

[6] K. Maruyama, F. Nori, and V. Vedral, Colloquium: The physics of Maxwell's demon and information, Rev. Mod. Phys. 81, 1 (2009).

[7] L. Del Rio, J. Åberg, R. Renner, O. Dahlsten, and V. Vedral, The thermodynamic meaning of negative entropy, Nature (London) 474, 61 (2011).

[8] S. Toyabe, T. Sagawa, M. Ueda, E. Muneyuki, and M. Sano, Experimental demonstration of information-to-energy conversion and validation of the generalized Jarzynski equality, Nat. Phys. 6, 988 (2010).

[9] C. Elouard, D. Herrera-Martí, B. Huard, and A. Auffeves, Extracting Work from Quantum Measurement in Maxwell's Demon Engines, Phys. Rev. Lett. 118, 260603 (2017).

[10] M. O. Scully, M. S. Zubairy, G. S. Agarwal, and H. Walther, Extracting work from a single heat bath via vanishing quantum coherence, Science 299, 862 (2003).

[11] F. Plastina, A. Alecce, T. J. G. Apollaro, G. Falcone, G. Francica, F. Galve, N. LoGullo, and R. Zambrini, Irreversible Work and Inner Friction in Quantum Thermodynamic Processes, Phys. Rev. Lett. 113, 260601 (2014).

[12] R. Uzdin, A. Levy, and R. Kosloff, Equivalence of Quantum Heat Machines, and Quantum-Thermodynamic Signatures, Phys. Rev. X 5, 031044 (2015).

[13] J. Goold, M. Huber, A. Riera, L. Del Rio, and P. Skrzypczyk, The role of quantum information in thermodynamics — a topical review, J. Phys. A 49, 143001 (2016).

[14] G. Benenti, G. Casati, K. Saito, and R. S. Whitney, Fundamental aspects of steady-state conversion of heat to work at the nanoscale, Phys. Rep. **694**, 1 (2017).

[15] M. Esposito, U. Harbola, and S. Mukamel, Nonequilibrium fluctuations, fluctuation theorems, and counting statistics in quantum systems, Rev. Mod. Phys. **81**, 1665 (2009).

[16] M. Campisi, P. Hänggi, and P. Talkner, Colloquium: Quantum fluctuation relations: Foundations and applications, Rev. Mod. Phys. **83**, 771 (2011).

[17] P. Sgroi, G. M. Palma, and M. Paternostro, Reinforcement Learning Approach to Nonequilibrium Quantum Thermodynamics, Phys. Rev. Lett. **126**, 020601 (2021).

[18] K. Micadei, G. T. Landi, and E. Lutz, Quantum Fluctuation Theorems Beyond Two-Point Measurements, Phys. Rev. Lett. **124**, 090602 (2020).

[19] M. Lostaglio, Quantum Fluctuation Theorems, Contextuality, and Work Quasiprobabilities, Phys. Rev. Lett. **120**, 040602 (2018).

[20] Y. Zou, Y. Jiang, Y. Mei, X. Guo, and S. Du, Quantum Heat Engine Using Electromagnetically Induced Transparency, Phys. Rev. Lett. **119**, 050602 (2017).

[21] Q. Bouton, J. Nettersheim, S. Burgardt, D. Adam, E. Lutz, and A. Widera, A quantum heat engine driven by atomic collisions, Nat. Commun. **12**, 2063 (2021).

[22] N. Van Horne, D. Yum, T. Dutta, P. Hänggi, J. Gong, D. Poletti, and M. Mukherjee, Single-atom energy-conversion device with a quantum load, npj Quantum Inf. **6**, 37 (2020).

[23] J. Klatzow, J. N. Becker, P. M. Ledingham, C. Weinzetl, K. T. Kaczmarek, D. J. Saunders, J. Nunn, I. A. Walmsley, R. Uzdin, and E. Poem, Experimental Demonstration of Quantum Effects in the Operation of Microscopic Heat Engines, Phys. Rev. Lett. **122**, 110601 (2019).

[24] K. Ono, S. Shevchenko, T. Mori, S. Moriyama, and F. Nori, Analog of a Quantum Heat Engine using a Single-Spin Qubit, Phys. Rev. Lett. **125**, 166802 (2020).

[25] G. L. Zanin *et al.*, Enhanced photonic Maxwell's demon with correlated baths, arXiv:2107.09686.

[26] J. V. Koski, V. F. Maisi, T. Sagawa, and J. P. Pekola, Experimental Observation of the Role of Mutual Information in the Nonequilibrium Dynamics of a Maxwell Demon, Phys. Rev. Lett. **113**, 030601 (2014).

[27] J. V. Koski, V. F. Maisi, J. P. Pekola, and D. V. Averin, Experimental realization of a Szilard engine with a single electron, Proc. Natl. Acad. Sci. U.S.A. **111**, 13786 (2014).

[28] J. V. Koski, A. Kutvonen, I. M. Khaymovich, T. Ala-Nissila, and J. P. Pekola, On-chip Maxwell's Demon as an Information-Powered Refrigerator, Phys. Rev. Lett. **115**, 260602 (2015).

[29] G. Manzano, D. Subero, O. Maillet, R. Fazio, J. P. Pekola, and E. Roldan, Thermodynamics of Gambling Demons, Phys. Rev. Lett. **126**, 080603 (2021).

[30] P. A. Camati, J. P. S. Peterson, T. B. Batalhao, K. Micadei, A. M. Souza, R. S. Sarthour, I. S. Oliveira, and R. M. Serra, Experimental Rectification of Entropy Production by Maxwell's Demon in a Quantum System, Phys. Rev. Lett. **117**, 240502 (2016).

[31] J. P. Peterson, T. B. Batalhao, M. Herrera, A. M. Souza, R. S. Sarthour, I. S. Oliveira, and R. M. Serra, Experimental Characterization of a Spin Quantum Heat Engine, Phys. Rev. Lett. **123**, 240601 (2019).

[32] R. J. de Assis, T. M. deMendonca, C. J. Villas-Boas, A. M. deSouza, R. S. Sarthour, I. S. Oliveira, and N. G. deAlmeida, Efficiency of a Quantum Otto Heat Engine Operating under a Reservoir at Effective Negative Temperatures, Phys. Rev. Lett. **122**, 240602 (2019).

[33] N. Cottet, S. Jezouin, L. Bretheau, P. Campagne-Ibarcq, Q. Ficheux, J. Anders, A. Auffèves, R. Azouit, P. Rouchon, and B. Huard, Observing a quantum Maxwell demon at work, Proc. Natl. Acad. Sci. U.S.A. **114**, 7561 (2017).

[34] G. Manzano, F. Plastina, and R. Zambrini, Optimal Work Extraction and Thermodynamics of Quantum Measurements and Correlations, Phys. Rev. Lett. **121**, 120602 (2018).

[35] L. Bresque, P. A. Camati, S. Rogers, K. Murch, A. N. Jordan, and A. Auffeves, Two-Qubit Engine Fueled by Entanglement and Local Measurements, Phys. Rev. Lett. **126**, 120605 (2021).

[36] S. Seah, S. Nimmrichter, and V. Scarani, Maxwell's Lesser Demon: A Quantum Engine Driven by Pointer Measurements, Phys. Rev. Lett. **124**, 100603 (2020).

[37] K. V. Hovhannisyan, M. Perarnau-Llobet, M. Huber, and A. Acín, Entanglement Generation is not Necessary for Optimal Work Extraction, Phys. Rev. Lett. **111**, 240401 (2013).

[38] M. Perarnau-Llobet, K. V. Hovhannisyan, M. Huber, P. Skrzypczyk, N. Brunner, and A. Acin, Extractable Work from Correlations, Phys. Rev. X **5**, 041011 (2015).

[39] B. Karimi and J. Pekola, Otto refrigerator based on a superconducting qubit: Classical and quantum performance, Phys. Rev. B **94**, 184503 (2016).

[40] K. Brandner and U. Seifert, Periodic thermodynamics of open quantum systems, Phys. Rev. E **93**, 062134 (2016).

[41] J. P. Pekola, B. Karimi, G. Thomas, and D. V. Averin, Supremacy of incoherent sudden cycles, Phys. Rev. B **100**, 085405 (2019).

[42] K. Beyer, K. Luoma, and W. T. Strunz, Steering Heat Engines: A Truly Quantum Maxwell demon, Phys. Rev. Lett. **123**, 250606 (2019).

[43] L. Szilárd, Über die entropieverminderung in einem thermodynamischen system bei eingriffen intelligenter wesen, Z. Phys. **53**, 840 (1929).

[44] L. Szilárd, On the decrease of entropy in a thermodynamic system by the intervention of intelligent beings, Behav. Sci. **9**, 301 (1964).

[45] J. Dunkel, Engines and demons, Nat. Phys. **10**, 409 (2014).

[46] M. Ribezzi-Crivellari and F. Ritort, Large work extraction and the Landauer limit in a continuous Maxwell demon, Nat. Phys. **15**, 660 (2019).

[47] A. Bérut, A. Arakelyan, A. Petrosyan, S. Ciliberto, R. Dillenschneider, and E. Lutz, Experimental verification of Landauer's principle linking information and thermodynamics, Nature (London) **483**, 187 (2012).

[48] B. Morris, L. Lami, and G. Adesso, Assisted Work Distillation, Phys. Rev. Lett. **122**, 130601 (2019).

[49] R. Uola, A. C. S. Costa, H. C. Nguyen, and O. Gühne, Quantum steering, Rev. Mod. Phys. **92**, 015001 (2020).

[50] F. Dolde *et al.*, High-fidelity spin entanglement using optimal control, Nat. Commun. **5**, 3371 (2014).

[51] X. Rong, J. Geng, F. Shi, Y. Liu, K. Xu, W. Ma, F. Kong, Z. Jiang, Y. Wu, and J. Du, Experimental fault-tolerant

universal quantum gates with solid-state spins under ambient conditions, Nat. Commun. **6,** 8748 (2015).

[52] Z. Li, Z. Chai, Y. Guo, W. Ji, M. Wang, F. Shi, Y. Wang, S. Lloyd, and J. Du, Resonant quantum principal component analysis, Sci. Adv. **7,** eabg2589 (2021).

[53] P. Neumann, J. Beck, M. Steiner, F. Rempp, H. Fedder, P. R. Hemmer, J. Wrachtrup, and F. Jelezko, Single-shot readout of a single nuclear spin, Science **329,** 542 (2010).

[54] L. Robledo, L. Childress, H. Bernien, B. Hensen, P. F. A. Alkemade, and R. Hanson, High-fidelity projective read-out of a solid-state spin quantum register, Nature (London) **477,** 574 (2011).

[55] Q. Zhang *et al.*, High-fidelity single-shot readout of single electron spin in diamond with spin-to-charge conversion, Nat. Commun. **12,** 1529 (2021).

[56] See Supplemental Material at http://link.aps.org/supplemental/10.1103/PhysRevLett.128.090602 for details in the work extraction operations, the local work extraction bounds and the experimental implementation, which includes Ref. [57].

[57] V. Jacques, P. Neumann, J. Beck, M. Markham, D. Twitchen, J. Meijer, F. Kaiser, G. Balasubramanian,

F. Jelezko, and J. Wrachtrup, Dynamic Polarization of Single Nuclear Spins by Optical Pumping of Nitrogen-Vacancy Color Centers in Diamond at Room Temperature, Phys. Rev. Lett. **102,** 057403 (2009).

[58] S. J. Jones, H. M. Wiseman, and A. C. Doherty, Entanglement, Einstein-Podolsky-Rosen correlations, Bell nonlocality, and steering, Phys. Rev. A **76,** 052116 (2007).

[59] R. F. Werner, Quantum states with Einstein-Podolsky-Rosen correlations admitting a hidden-variable model, Phys. Rev. A **40,** 4277 (1989).

[60] D. J. Saunders, S. J. Jones, H. M. Wiseman, and G. J. Pryde, Experimental EPR-steering using Bell-local states, Nat. Phys. **6,** 845 (2010).

[61] T. Feng *et al.*, Steering paradox for Einstein–Podolsky–Rosen argument and its extended inequality, Photonics Res. **9,** 992 (2021).

[62] S. Designolle, V. Srivastav, R. Uola, N. H. Valencia, W. McCutcheon, M. Malik, and N. Brunner, Genuine High-Dimensional Quantum Steering, Phys. Rev. Lett. **126,** 200404 (2021).